Non-canonically regulated heterochronic expression of Hsp70 drives clonal expansion and invasion in *Drosophila* epithelial tumors

Abhijit Biswas[1]*, Gunjan Singh[2,3]*, Vishal Arya[1], Subhash Chandra Lakhotia[1] and Devanjan Sinha[1$]

[1]Cytogenetics Laboratory, Department of Zoology, Institute of Science, Banaras Hindu University, Varanasi – 221005, Uttar Pradesh, India

[2,3]Present Address: Department of Molecular Biology, Cell Biology, & Biochemistry, and Department of Neuroscience, Brown University, Providence, RI, USA

*The authors contributed equally to this work.

[$]To whom correspondence should be addressed:

Dr. Devanjan Sinha
Cytogenetics Laboratory,
Department of Zoology,
Institute of Science, Banaras Hindu University,
Varanasi – 221005, Uttar Pradesh, India

This work is the revised version of the bioRxiv preprint:
https://doi.org/10.1101/2023.02.02.526918

Abstract

Tumour progression is orchestrated by a complex interplay of genetic, epigenetic, and microenvironmental cues, with increasing recognition of the role of stress response pathways in modulating clonal dynamics. Among these, the evolutionarily conserved heat shock protein, Hsp70 has emerged as a key regulator of tumour cell survival and proliferation, but with poorly defined regulatory control. Using *Drosophila* wing epithelium as a model, we found that lgl^{4} yki^{OE} MARCM clones developing into malignant tumours showed characteristic by spatio-temporal elevation of Hsp70 which correlated with enlarged clonal volume and invasive dissemination. Hsp70 upregulation was independent of canonical stress-response regulators such as Heat Shock Factor (HSF) and Hif1α. Instead, ROS-mediated activation of JNK triggered downstream activation of dFOXO, which in turn drove Hsp70 expression. Knockdown of *Nox*, a major ROS producer, or genetic inhibition of JNK signaling abrogated Hsp70 induction and curtailed tumour expansion, underscoring a non-canonical, redox-dependent mechanism of Hsp70 regulation. Collectively, these findings position Hsp70 as a temporally dynamic, ROS-JNK-FOXO axis-dependent driver of neoplastic transformation. The unusual regulatory dynamics of Hsp70 reveal a unique mode of tumour fitness, heterogeneity and an atypical control logic for a conserved chaperone, having future prognostic implications in mammalian epithelial carcinomas.

Introduction

Tumorigenesis is defined by presence of a multifarious patterns of cellular diversity, driven by clonal selection and proliferation. These clonal populations progressively diverge genetically, transcriptionally, and proteomically, enabling them to achieve varying levels of fitness[1,2]. In the multi-step process of tumour development, the prevailing view is that somatic mutations in a single cell provide clonal advantages, facilitating its expansion and the subsequent accumulation of additional genetic and epigenetic lesions. Over time, these mutant cells outcompete neighbouring cells, evolving into a heterogeneous mass of invasive populations[3,4]. This acquisition of the neoplastic phenotype is primarily an adaptive response to intrinsic and extrinsic pressures[5].

The adaptive features include numerical and structural variations in the chromatin, epigenetic modifications, inflammation, metabolic reprogramming and single nucleotide variants[6-11]. Chromosomal abnormalities, causing loss of tumour suppressors, oncogenic fusions or copy number variations in oncogenes, elicit large scale changes in gene expression profiles. While modifications in epigenetic marks and classical cancer mutations influence tumour evolutionary dynamics, many of these changes are tolerable in normal tissues, raising questions about additional factors promoting malignancy[12]. A recent pan-cancer analysis by ICGC/TCGA whole genomes consortium indicated that around 5% of the cancer cases did not contain any identifiable driver mutations. An emerging perspective posits that mutations alone are insufficient for cancer progression, necessitating other molecular prerequisites[13]. One of the drivers of cancer progression is the common over-expression of the chaperone family of stress proteins[14,15], which adapts the cancer cells to stresses originating intrinsically or from the tumour microenvironment. However, their precise consequential implications and regulation remain underexplored.

Hsp70 is highly conserved in both prokaryotes and eukaryotes, mainly functioning in protein quality control mechanisms of the cells. It is overexpressed in most cancers and is mechanistically implicated in tumor development by enabling cells to withstand stressors such as nutrient deprivation, hypoxia and low pH[16-18]. Emerging evidences highlight its involvement in dysregulating multiple oncogenic pathways, including receptor tyrosine kinases, Ras, and the Akt-mTOR pathway[19-23]. Hsp70 also suppresses apoptosis by preventing the activation of pro-apoptotic signals and formation of the apoptosome[20,24-29]. Given its extensive role in cancer development and progression, Hsp70 has long been considered a promising therapeutic

target[30-32]. However, a clinically approved protocol remains elusive[33,34], partly due to limited understanding of its expression patterns in developing tumours, and the regulatory factors involved.

Previous work from our lab had shown constitutive elevation of heat shock proteins in tumour backgrounds except for Hsp70 whose expression was regionally restricted[35]. The present work identifies a non-canonical temporal induction of Hsp70 as a major driver of the proliferative phenotype. Using *Drosophila* genetic models of tumorigenesis[36], we observed undetectable Hsp70 levels during the early development of tumor clones. However, its expression temporally increased, with isolated Hsp70-positive cells gradually expanding spatially to most of the clonal cells which correlated with enhanced clonal size and invasive phenotypes. Depleting or inhibiting Hsp70 significantly slowed tumor growth, reduced expression of the invasive markers and improved host's survivability. Interestingly, induction of Hsp70 in tumor clones was independent of the canonical transcription factor HSF and hypoxia. Instead, the cellular redox state appears to be a critical regulator, with FOXO mediating Hsp70 induction. Our findings provide evidence that Hsp70 acts as one of the causal drivers of tumour growth and highlights its redox-dependent regulation which offers new avenues for therapeutic intervention targeting this protein.

Results:

Spatio-temporal pattern of Hsp70 expression correlates with growth of tumour clones

Heat Shock Proteins (HSPs) are known to enable cancer cells tolerate various intra- and extra-cellular stresses faced by expanding cancer cell population and are hence constitutively overexpressed across the tumour landscape. Meta-analysis of Hsp70 expression across pan-cancer datasets from the TCGA database revealed elevated levels of the protein in multiple tumour types compared to corresponding normal tissues (Fig S1A). This upregulation correlated with higher tumour grades in specific tumour types (Fig S1B and C), suggesting a role for Hsp70 in progression of these tumours. Moreover, patients with low Hsp70 expression exhibited improved overall survival across several carcinoma types (Fig S1D-G). These data and others in the available literature, however, do not provide information about the temporal order of Hsp70 expression.

Taking advantage of a *Drosophila* model of tumourigenesis for temporally following the growth of a tumour, our study delineated a causal role of Hsp70 in tumour growth and regulation of its expression in MARCM genetic model of epithelial tumour. In agreement with earlier report form our laboratory[35], we confirmed that developmentally expressing HSPs like Hsp60, Hsc70 and Hsp83 were ubiquitously elevated in lgl^4 yki^{OE} tumour clones (Fig S1H). In contrast, Hsp70 was not detectable during early stages of establishment of clones but appeared at 72 h after clone induction (ACI), exhibiting a sporadic expression pattern (FigS1H).

A progressive increase in Hsp70 expressing cells was noted between 72 to 144 h ACI, in parallel with increase in clone size (Fig. 1A-D). At 72 h ACI, only ~25 % of tumour clones were positive for Hsp70 expression, with the frequency of $Hsp70^+$ clones increasing to 30%, 42% and 90% at 96 h, 120 h and 144 h ACI, respectively (Fig. 1E). Correspondingly, the proportion of the GFP^+ tumor area occupied by $Hsp70^+$ cells increased from 15% at 72 h ACI to 80% at 144 h ACI (Fig. 1A-D and I). This was accompanied by a parallel rise in Hsp70 fluorescence intensity and an overall expansion in tumour size (Fig. 1F). Depletion of Hsp70 in lgl^4 yki^{OE} tumour clones through co-expression of *hsp70-RNAi* transgene resulted in overall reduction in sizes of lgl^4 yki^{OE} clones (Fig. 1G-I and J-K); indicating that expansion of $Hsp70^+$ cells paralleled enhanced rate of tumour growth (Fig. 1L).

Depletion of Hsp70 compromises proliferative and migratory capacity of tumour

All further analysis were performed with wing discs carrying 72 h old lgl^4 yki^{OE} clones, which corresponded to early stage of Hsp70 expression. The enlarged size of lgl^4 yki^{OE} tumour clones was associated with high proliferative activity, as evidenced by an increased number of phospho-Histone H3 $(pH3)^+$ mitotic nuclei in the clonal areas (Fig. 2A and C). Depletion of Hsp70 led to a reduction in $pH3^+$ nuclei that correlated with a significant decrease in clone size (Fig. 2B and C). RNAi mediated reduction of Hsp70 was also associated with increased expression of the pro-apoptotic marker Dcp1 in tumourous clones (Fig. 2D-F), and an enhanced developmental progression of the tumour carrying larvae. Following tumour induction, most larvae form pseudopupae or die at pharate stages, with only ~50% successfully emerging as adults. Hsp70 downregulation substantially improved their survival so that ~70% of the lgl^4 yki^{OE} clone carrying larvae successfully emerged as adults (Fig. 2G).

The phenotypic rescue achieved through *hsp70-RNAi* was further confirmed by treating the lgl^4 yki^{OE} clone carrying larvae with Hsp70 inhibitor, Pifithrin-μ[37], which not only reduced the size

of the tumour clones at 72h and 96h ACI (Fig. 2H-J and S2A-C), but also improved the survivability of these larvae as most of them successfully developed to adult stage (Fig. 2K). The observed rescue of *lgl*^{4} *yki*^{OE} clone carrying larvae was not due to reduction in expression of Hsp70 but through reported inhibition of its function by Pifithrin-μ's binding with nucleotide binding domain[38] (Fig. S2D-E). Besides the improved survival of *lgl*^{4} *yki*^{OE} clone carrying larvae to adult stage, the frequencies of tumourous nodules in different appendages of adult flies (Fig. 2L) also decreased following down-regulation of Hsp70 (Fig. 2M).

In addition to diminishing proliferative capacity, Hsp70 depletion also appeared to impair the migratory and invasive properties of tumourous cells. A readout of the aggressive and invasive behaviour, is high accumulation of matrix metalloproteinase 1 (MMP1), whose levels was high in 72 h old *lgl*^{4} *yki*^{OE} clones. MMP1 levels were markedly reduced upon Hsp70 knockdown (Fig. 3A-C) or pharmacological inhibition of Hsp70 by Pifithrin-μ (Fig. S3A-B and D), along with comparable reduction is clone size (Fig. 3D and S3C). Among *lgl*^{4} *yki*^{OE} cells, those expressing Hsp70 displayed considerable cytoplasmic edge extensions (Fig. 3E) and unidirectional F-actin polymerization/lamellipodia formation (Fig. 3F-H), indicative of enhanced migratory ability. The relative edge extensions and morphological distortions were comparatively more in Hsp70^{+} cells, compared to their Hsp70 negative counterparts (Fig. 3H).

Hsp70 is essential for sustaining tumour growth and invasiveness in allografted tissue

Allografting tumour tissue into a healthy adult *Drosophila* has long served as the gold standard for evaluating tumourigenicity[39-41]. To validate the observed correlation between Hsp70 expression and tumour growth, we assessed whether the primary tumours retained similar proliferative and invasive behaviour in an allogeneic environment. Tumour bearing imaginal discs from *lgl*^{4} *yki*^{OE} and *lgl*^{4} *yki*^{OE}; *hsp70*^{RNAi} larvae were dissected at 96 h ACI and transplanted into the abdomens of 2 days old adult wild type (*OregonR*$^{+}$) female flies (Fig. 4A). Post-transplantation, host flies were maintained at 24°C±1 and monitored overtime. In *lgl*^{4} *yki*^{OE} allografts, the GFP signal from the tumour clones increased progressively from 3 to 14 days assay duration (Fig. 4E and H), indicating sustained tumour expansion. In contrast, *lgl*^{4} *yki*^{OE}; *hsp70*^{RNAi} allografts exhibited minimal growth with limited GFP signal, and growth of the GFP foci remained more or less stunted for even at the terminal stages of observation (Fig. 4F and H). The aggressive tumour growth in *lgl*^{4} *yki*^{OE} grafts often resulted in abdominal distension due to fluid accumulation and tumour spread (Fig. 4B and G), whereas hsp*70*^{RNAi} grafts did not

induce the abdominal inflation of *lgl*^{4} *yki*^{OE} grafts and showed close to normal abdominal morphology similar to control disc grafts (Fig. 4C-D and G). Immunofluorescent imaging of host abdomen revealed extensive invasion of *lgl*^{4} *yki*^{OE} tumour cells into adjacent tissues, supported by dense F-actin networks (Fig. 4I-J). Notably, Hsp70-positive clones also showed evidence of distal invasion (Fig. 4K). Collectively, these findings reinforce Hsp70 as a critical determinant of tumor clonal growth and invasiveness in the *lgl*^{4} *yki*^{OE} background, and its depletion markedly impairs these malignant properties.

HSF is not responsible for Hsp70 induction in *lgl*^{4} *yki*^{OE} clones

As a part of evolutionary well-conserved response, heat shock proteins are generally induced by stressed cells by activated transcription factor, HSF[42]. Elevated levels of HSF are associated with prooncogenic processes in different mammalian tumours and causes induction of multiple molecular chaperones[43]. Moreover, baseline expression of constitutively expressing heat shock proteins is expectedly HSF independent[35], unlike Hsp70 which is stress-inducible and appears after establishment of tumour clones. Therefore, we examined expression of Hsp70 in *lgl*^{4} *yki*^{OE}*;hsf*^{RNAi} background. The HSF expression was relatively similar among *lgl*^{4} *yki*^{OE} clonal and non-clonal cells (Fig. 5A-B and C), and upon *hsf*^{RNAi} clone-specific knock-down was achieved (Fig. 5A-B and D-E). Despite effective reduction of HSF in the clones, the magnitude of Hsp70 expression remained unaltered (Fig. 5A-B and F-G) and tumour size showed no significant variation (Fig. 5H). Consequently, *hsf*^{RNAi} did not rescue the poor survivability associated with *lgl*^{4} *yki*^{OE} tumours (Fig. 5I). These results indicated that Hsp70 expression in these tumours is independent of HSF, implicating possible involvement of alternative non-canonical transcriptional regulators.

Non-canonical regulation of Hsp70 implicates FOXO as a key upstream driver

Given the prominent role of hypoxia response as one of the major drivers of tumour progression[44,45], we tested the potential involvement of Hif1α (Sima in fruit flies) in induction of Hsp70, since it has a binding site at Hsp70 promoter[46]. Depletion of Sima under *lgl*^{4} *yki*^{OE} background by co-expressing *sima-RNAi* transgene, did not cause any significant alteration in Hsp70 expression, spatial distribution and clonal growth (Fig. S4A-E). Finally, we investigated the role of the transcription factor FOXO, proposed to bind the presumptive Forkhead-

responsive element (FRE) in Hsp70 promoter[47]. Notably, Hsp70+ cells within *lgl*^{4} *yki*^{OE} tumour clones displayed high FOXO levels, suggesting a functional correlation (Fig. 5J). Downregulation of FOXO in the *lgl*^{4} *yki*^{OE} tumours resulted in a significant reduction of Hsp70 expression and clonal area (Fig. 5K-O). Hence, *lgl*^{4} *yki*^{OE}*; foxo*^{RNAi} larvae showed better developmental survivability with more than 70% of them emerging into adults (Fig. 5P). The above observations further supported by reanalysis of publicly available RNAseq data from *Nubbin-Gal4>UAS-yki*^{S168A} tumours[48] that revealed co-upregulation of *foxo*, *yki*, and *Mmp1*, enrichment of associated signaling pathways, and a concurrent downregulation of *sima* and *hsf* (Fig. S4F-G). These results indicate that under activated Yki background, expression of Hsp70 is regulated non-canonically by FOXO.

Redox-mediated JNK–FOXO axis drives Hsp70 expression and tumour expansion

The functional state of FOXO is regulated by upstream kinases- Akt and JNK[49,50]. While Akt suppresses the tumor-suppressive activities of FOXO via phosphorylation and cytoplasmic retention, JNK promotes FOXO activation under stress conditions[49]. To examine this regulatory dichotomy, we treated *lgl*^{4} *yki*^{OE} tumour-bearing larvae with Capivasertib, a selective Akt inhibitor[51]. Although a marginal increase in clonal size was observed (Fig. 6A-C), Hsp70 expression levels and distribution remained unaffected (Fig. 6A-B, D and E). The phenotypes suggested that FOXO activation and subsequent Hsp70 induction may be largely independent of Akt signaling in this context. To probe the involvement of JNK, we expressed a dominant-negative allele of *basket* (*bsk*^{DN}, the *Drosophila* mutant allele of JNK) within *lgl*^{4} *yki*^{OE} clones. Introduction of this allele markedly reduced the number of Hsp70^{+} tumour cells and overall Hsp70 expression (Fig. 6F-G and I-J), which was accompanied by significant clonal growth impairment (Fig. 6H). As a result, over 80% of larvae harboring *lgl*^{4} *yki*^{OE}; *bsk*^{DN} clones successfully developed into adults (Fig. S5A). The observation was further supported by co-localization of elevated pJNK with Hsp70-rich zones, underscoring a spatial correlation between JNK activation and Hsp70 induction (Fig. 7A and A' *bounded boxes*).

To identify upstream regulators of JNK activation and subsequent FOXO-driven Hsp70 expression and tumour growth, we assessed the role of redox state which is known to have a bearing on tumour growth. NADPH oxidase (Nox), a major source of reactive oxygen species (ROS), is often dysregulated in various tumours, promoting malignant behaviour[52]. Therefore, we targeted Nox via RNAi in *lgl*^{4} *yki*^{OE} background. The *nox*^{RNAi} clones exhibited substantially

reduced expression of Hsp70 (Fig. 7A'-B' and D-E) and impaired clonal growth (Fig. 7C), with improved survival to adult stage (Fig. 7G). The tumours also showed lower levels of pJNK (Fig 7A-B), indicating possible ROS mediated activation of the protein. The Glutathione homeostasis, that acts as a redox buffer, has been observed to be a key regulator of JNK activation[53-55]. Treatment with buthionine sulfoximine (BSO), an inhibitor of GSH synthesis, elevated pJNK and Hsp70 levels (Fig. 7K-M), which colocalized within tumour clones (Fig. S6A-B) and corresponded with proportionate expansion of tumour clones (Fig. 7H-J). Conversely, supplementation with N-acetylcysteine (NAC), a precursor of GSH[56] and a potent antioxidant, led to marked reduction in clonal size and downregulation of Hsp70 expression pattern (Fig. S6C-G). Collectively, these finding demonstrate redox-sensitive activation of Hsp70 through JNK-FOXO axis that result in gradual expansion of tumour clones.

Discussion

In the competitive tumour landscape, dynamic changes in gene expression profiles determine tumour growth and metastasis. Besides transcription regulators, certain proteins act as drivers of tumour development. Our results suggest that the stress-inducible Hsp70 may play such role in epithelial tumours in *Drosophila.* The 70 kDa heat shock protein family includes the constitutively expressing Hsc70 and stress-inducible Hsp70[23,57,58]. Normally, Hsp70 is maintained at very low levels but its expression is highly induced under proteotoxic conditions such as heat, hypoxia and non-permissive pHs[17,46,57,59].

The expression of Hsp70 in tumors is prognostically significant and positive correlation has been demonstrated between the protein and patient survivability[34,60,61]. Several studies have proposed a role of Hsp70 in malignant transformation through prevention of apoptosis, modulation of inflammatory, oncogenic pathways [19,23,34,62]. Cancer cells depleted for Hsp70 presented senescent morphological features and cell cycle arrest[21]. Hsp70's pro-tumourigenic function may derive from its interactions with several factors associated with cell growth. Hsp70 plays a positive role in regulating Ras-Erk activation and Hsp70 family members are thought to indirectly promote Erk expression[16,22]. Haploinsufficiency or knock-down of Hsp70 reduced KRas levels and caused suppression of lung and pancreatic tumours [63,64]. Hsp70 members in general are known to facilitate PI3K/Akt/mTOR, promoting cancer progression[18,65-67]. Removal of Hsp70 from the tumour clones lowered the active forms of these factors and made the cells more prone to apoptosis.

We provided insights on the regulatory dynamics of Hsp70 in tumour growth using *Drosophila* tumour models that has an advantage of being genetically stable with relative homogeneity[68]. The imaginal discs of *Drosophila*, made up epithelial cells organized in very specific patterns, can become tumourigenic following disruption of several different regulatory pathways similar to the mammalian epithelial cells[68]. It is significant that irrespective of the genetic background of tumourous clones induced in imaginal discs, Hsp70 expression followed a characteristic temporal and spatial expression pattern, which correlated with the tumour's proliferative and invasive behaviour. Loss of Hsp70 expression or its inhibition not only caused reduced tumour growth but also the cells failed to engraft and proliferate within normal tissue microenvironment, aligning with the concept of Hsp70 being the driver of malignancy. In this context it is notable that Hsp70 is required for the normal border cell migration in the Drosophila ovary[69].

Expression of Hsp70 is normally driven by activated HSF following exposure of cells to stress. Particularly in cancer cells, induction of HSF is important in maintaining high levels of molecular chaperones required to counter to proteomic imbalance brought about by genomic alterations and stress[70,71]. In addition, HSF is also known to induce transcriptional programs associated with malignant transformation [44,45]. HSF is known to modulate the expression of Hif1α, the master regulator of cellular response to hypoxia, that also induces Hsp70 expression[72,73]. Contrary to the known role of HSF as the major regulator of stress-induced Hsp70, our results indicate that expression of Hsp70 in $lgl^{4}\ yki^{OE}$ tumours to be independent of both HSF and Hif1α (Sima), as depleting either of the proteins did not affect Hsp70 expression and tumour growth. The characteristic spatio-temporal expression pattern of Hsp70, that enhanced the tumour fitness, was found to be dependent on FOXO in $lgl^{4}\ yki^{OE}$ tumours and regulated by the cellular redox state. FOXO family of transcription factors are associated with multiple cellular processes such as cell cycle arrest, apoptosis, autophagy, DNA repair, through which it exerts its tumour modulatory effect[74,75]. Under oxidative stress, JNK phosphorylates FOXO, leading to its activation and nuclear translocation[49,50]. In ischemic mouse models, FOXO physically interacts with Yki (YAP) to regulate antioxidant defence[76]. In *scrib* Ras^{V12} model, lowering of ROS associates with reduction of tumour clones[77]. Loss of epithelial polarity regulators such *scrib, dlg, lgl* promote tumour through JNK under suppressed Hippo pathway[78]. Reduction of JNK activity, either by its depletion or by changing levels of reduced glutathione, resulted in loss of Hsp70 levels and concomitant reduction in tumour clones. These results were also phenocopied upon downregulating one of the cellular ROS generators, NADH

oxidases, or upon exposure to antioxidants. The cell growth driven by oxidative stress-mediated FOXO-dependent activation of Hsp70 supports the dual role for FOXO in regulating both cell proliferative and death pathways.

This study highlights the heterochronicity of Hsp70 expression among developing tumours, emphasizing on its role in enhancing cellular growth and sustenance within the tumour microenvironment. While other molecular chaperones are generally ubiquitously expressed across tumour landscapes[15,71], the spatio-temporal heterogeneity in Hsp70 expression observed here suggests this chaperone's unique functional requirements during tumour expansion. Our study raises several compelling questions: what clonal advantages are conferred by Hsp70 that enable certain cells to outcompete their neighbours? While reactive oxygen species (ROS) appear to be the key in inducing Hsp70, what determines its activation in only a subset of tumour cells? Do Hsp70-positive populations exhibit greater immune evasion or possess distinct metabolic traits, and is Hsp70 expression a driver or a consequence of these characteristics? While these questions remain open, our findings offer valuable insights into the expression dynamics of this critical chaperone in tumours. These findings pave the way for exploring innovative strategies for diagnosis and prognosis in mammalian systems, with potential implications for understanding and targeting tumour progression.

Materials and Methods:

***Drosophila* stocks and genetics:** All the fly stocks and crosses were maintained on standard fly food made up of yeast, sugar and agar-maize powder at 24 ± 1°C. The following fly stocks were used to set up crosses to obtain progeny of the desired genotypes:

1. *y 1.* w* *hsFLP tubGAL4 UAS-GFP; tubGAL80 FRT40A/CyO-GFP; +/+;* (Kind gift from Prof. Pradip Sinha, IIT Kanpur).

2. *w*; lgl^4 FRT40A yki^{OE} /CyO-GFP; +/+* (*lgl* mutant is referred to as lgl^4 and *UAS-yki* referred to as yki^{OE}); (Kind gift from Prof. Pradip Sinha, IIT Kanpur).

3. *y 1 sc* v 1 sev21*; P{y[+t7.7] v[+t1.8]=TRiP.GLV21028}attP2, (BDSC-35663; referred to as *hsp70 RNAi*).

4. *y1 v1; UAS-hsf-RNAi/TM3, Sb1*, (BDSC-27070, referred to as *hsf RNAi);*

5. *sc[*] v [1] sev[21]*; P{y[+t7.7]v[+t1.8]=TRiP.HMS00793}attP2 (BDSC-32993, referred to as *dfoxo RNAi*).

6. *y[1] sc[*] v[1] sev[21]*; P{y[+t7.7] v[+t1.8]=TRiP.HMS00691}attP2 (BDSC-32902, referred to as *nox-RNAi*).

7. *y[1] sc[*] v[1] sev[21]*; P{y[+t7.7] v[+t1.8]=TRiP.HMS00833}attP2 (BDSC-33895, referred to as *sima-RNAi*).

8. w[*]; P{w[+mC]=UAS-bsk.K53R}20.1a (BDSC-9311, referred to as bsk^{DN})

Tumour generation in *Drosophila* imaginal discs: For generation epithelial tumours in larval imaginal discs, Mosaic Analysis with a Repressible Cell Marker (MARCM) technique was used[79]. Tumour clones were generated by crossing the males of desired genotypes with virgin females from the MARCM stock (*y w hsFLP tubGAL4 UAS-GFP; FRT40A GAL80/CyO-GFP; +/+*) to create $lgl^4\ yki^{OE}$ or $lgl^4\ Ras^{V12}$ clones expressing alone or co-expressing with the desired transgene/mutant allele. MARCM clones of $lgl^4\ yki^{OE}$ or $lgl^4\ Ras^{V12}$ were generated essentially following Singh et. al.[35] Briefly, the clones were induced by exposing the early third instar larvae (72 h after egg laying (AEL)) to heat shock in a water bath at 37°C for 3 or 5 minutes respectively. The following fly genotypes were used:

1. *y w hsFLP tubGAL4 UAS-GFP; tubGAL80 FRT40A/* lgl^4Ras^{V12} *FRT40A; +/+*
2. *y w hsFLP tubGAL4 UAS-GFP; tubGAL80 FRT40A/* lgl^4yki^{OE} *FRT40A; +/+*
3. *y w hsFLP tubGAL4 UAS-GFP; tubGAL80 FRT40A/* lgl^4yki^{OE} *FRT40A; hsp70 RNAi/+*
4. *y w hsFLP tubGAL4 UAS-GFP; tubGAL80 FRT40A/* lgl^4yki^{OE} *FRT40A; hsf RNAi/+*
5. *y w hsFLP tubGAL4 UAS-GFP; tubGAL80 FRT40A/* lgl^4yki^{OE} *FRT40A; sima RNAi/+*
6. *y w hsFLP tubGAL4 UAS-GFP; tubGAL80 FRT40A/* lgl^4yki^{OE} *FRT40A; dfoxo RNAi/+*
7. *y w hsFLP tubGAL4 UAS-GFP; tubGAL80 FRT40A/* lgl^4yki^{OE} *FRT40A; nox RNAi/+*
8. *y w hsFLP tubGAL4 UAS-GFP; tubGAL80 FRT40A/* lgl^4yki^{OE} *FRT40A; UAS-*bsk^{DN}*/+*

Treatment of the larvae with different inhibitors: 500 µl yeast paste was prepared with 0.2g yeast powder, 10 µl food color (Green) and 200 mM of Pifithrin-µ (PFT-µ), Capivasertib [35 nM], N-acetyl cysteine (NAC) [2mg/ml] (Sigma-Aldrich, USA) or Butathione Sulfoximine (BSO) [200 mM]. Yeast paste was placed at the centre of Agar-petri plates. 20 lgl^4 yki^{OE} (48 h ACI) tumour bearing larvae were transferred to each petri-plates and kept at 24°C±1 for 24 h or 48 h, followed by dissection of wing imaginal discs. In case of survivability analysis, larvae were fed with the drugs from 48 h ACI till they pupated (varying between 1-2 days) and followed till either their death as pupae or emergence as adult flies. Respective control flies were fed with yeast paste without PFT-µ, Capivasertib, NAC or BSO supplementation, respectively.

Immunostaining and Confocal Microscopy: Imaginal discs of third instar larvae of appropriate genotypes and age (expressed as ACI for MARCM lines and days for other genotypes, as indicated in legends to figures) were dissected out in 1X Phosphate Buffer Saline (1X PBS) and immunostained following standard protocol[80]. The primary antibodies used for experiments were mouse anti-Hsp83 (1:50,3E6, a kind gift from Prof. Robert Tanguay) (Morcillo et al. 1993); rat anti-Hsp70 (7Fb 1:200, Sigma), rabbit anti-Hsp60 (1:50, CST-SP60, D307#4870), rabbit anti-PH3, mouse anti-MMP1 (1:50, DSHB-5H7B11), rabbit anti-Dcp1 (1:100, Cell Signaling, Asp-216); rabbit anti-pJNK (1:400, V7932 Promega, USA). rat anti-Hsp/Hsc70 (1:50, 3.701, a kind gift from Prof. S. Lindquist) (Velazquez and Lindquist, 1984), rabbit anti-HSF (a kind gift from Prof. J. T. Lis; 1:200), rabbit anti-dFoxo (1:200, ab195977, Abcam). Appropriate secondary antibodies conjugated with Alexa Fluor 546 or Alexa Fluor 633 (1:200, Molecular Probes, USA) were used. To stain DNA and F-actin, 6-diamidino-2-phenylindole dihydrochloride (DAPI, 1 µg/ml) and Phalloidin-633 (Atto) were used, respectively. Immunostained tissue were mounted with 1,4-Diazabicyclo [2.2.2] octane (DABCO) anti-fade mounting medium. All the immunostained images were collected with Zeiss LSM 900 confocal microscope using Plan-10X (0.45 NA), Apo 20X (0.8 NA) or 63X oil immersion (1.4 NA) objectives and Zeiss ZEN 3.4 Blue edition software. Quantitative analysis of the images was carried out using Fiji (Image-J). All the images shown here were assembled using Adobe Photoshop (2012). Statistical analysis of control and experimental samples were done through unpaired t-test in GraphPad Prism 8.4.2.

Survival assay: Larvae of the desired genotypes were allowed to develop till at 24°C±1. Numbers of those dying at early pupal (pseudopupae) or late pupal (pharate) stages and those

that emerged as adults were counted. GraphPad Prism 8.4.2 were used to check the statistical significance between the different datasets using Student's t-Test.

Transplantation of tumour discs: GFP positive tumor clone bearing wing imaginal disc were dissected out from *lgl*^{4} *yki*^{OE} *and lgl*^{4} *yki*^{OE}; *hsp70 RNAi* larvae (96 h ACI) in 70% Grace's Insect medium. Discs were fragmented with the help of insulin needle using a GFPscope (Vaiseshika/Plan 1X) and one fragment/fly was introduced into the abdomen of 2 days old virgin *Oregon R*+ females using a pulled glass capillary needle[81]. Injected host flies were kept in a food vial at 24°C±1 for further observation. GFP+ tumour growth within the host abdomen was imaged using a Nikon DS-Fi1c camera on a Nikon E800 Fluorescence microscope. 14 days post-transplantation, the host abdomens were dissected and immunostained using anti-Hsp70 and Phalloidin-633 as mentioned above.

Imaging of Adult flies: Photographs of tumour patches in different body parts of surviving adults and abdominal morphology of transplanted host flies were taken with Axio Cam Zeiss camera mounted on Nikon SMZ800N stereo-binocular microscope.

Analysis of RNAseq data: RNASeq data from an earlier published dataset (PMC id: PMC7768408) was reanalyzed to prepare a heat map showing differential expression of genes by SR plot. Gene sequence enrichment analysis was performed using Pangea.com. Significantly expressed genes were defined as those exhibiting an absolute fold-change of at least 1.5 and an FDR of less than or equal to 0.05.

Acknowledgement

We heartily thank Dr. Bama Charan Mandal, ISLS-BHU and CDC-BHU for Confocal microscope imaging system. We thank FIST-lab Zoology Dept. BHU for the central instrumentation facility. We heartily thank Prof. Pradip Sinha (IIT Kanpur, India) and Bloomington Drosophila Stock Centre (USA) for sharing the fly stocks with us. We share heartfelt gratitude to Prof. John. T. Lis (USA), Prof. Robert Tanguay (Canada), late Prof. S. Lindquist for sharing different antibodies, as mentioned in Materials and Methods. We also thank Prof. Mousumi Mutsuddi (MHG-BHU) for sharing micro-injector and glass capillary used in tumour transplantation.

Funding

This work is Indian Council of Medical Research Ad-hoc grant (5/13/87/2020/NCD-III), BHU-Institute of Eminence grant (R/Dev/IoE/Incentive/2021-22/32452) (to D.S.). The authors also acknowledge financial support from CSIR doctoral fellowship (to A.B.) and UGC doctoral fellowship (to G.S. and V.A.) and Science and Engineering Research Board (SB/DF/009/2019) (to S.C.L).

Author contributions

G.S., D.S., S.C.L. conceived the study. G.S. and A.B. designed experiments. Following generation of initial data by G.S., A.B. performed further experiments and analysed the data. V.A. performed the meta-analysis of TCGA datasets. D.S. framed the manuscript and wrote it with the help of S.C.L and A.B.. D.S. and S.C.L. funded the research.

Declaration of interest

The authors declare no competing interests

Data availability

The data that support the findings of this study are available within the main text and its Supplementary Information file. The lead contact will share all raw data associated with this paper upon reasonable request and, when applicable, fulfilment of appropriate material transfer agreements.

References

1 Berenblum, I. & Shubik, P. A new, quantitative, approach to the study of the stages of chemical cartinogenesis in the mouse's skin. *Br J Cancer* **1**, 383-391, doi:10.1038/bjc.1947.36 (1947).

2 Vogelstein, B. & Kinzler, K. W. The Path to Cancer --Three Strikes and You're Out. *N Engl J Med* **373**, 1895-1898, doi:10.1056/NEJMp1508811 (2015).

3 Hanahan, D. & Weinberg, R. A. Hallmarks of cancer: the next generation. *Cell* **144**, 646-674, doi:10.1016/j.cell.2011.02.013 (2011).

4 Merlo, L. M., Pepper, J. W., Reid, B. J. & Maley, C. C. Cancer as an evolutionary and ecological process. *Nat Rev Cancer* **6**, 924-935, doi:10.1038/nrc2013 (2006).
5 Janiszewska, M. The microcosmos of intratumor heterogeneity: the space-time of cancer evolution. *Oncogene* **39**, 2031-2039, doi:10.1038/s41388-019-1127-5 (2020).
6 Chang, J. *et al.* Genomic alterations driving precancerous to cancerous lesions in esophageal cancer development. *Cancer Cell* **41**, 2038-2050 e2035, doi:10.1016/j.ccell.2023.11.003 (2023).
7 Denk, D. & Greten, F. R. Inflammation: the incubator of the tumor microenvironment. *Trends Cancer* **8**, 901-914, doi:10.1016/j.trecan.2022.07.002 (2022).
8 Pavlova, N. N., Zhu, J. & Thompson, C. B. The hallmarks of cancer metabolism: Still emerging. *Cell Metab* **34**, 355-377, doi:10.1016/j.cmet.2022.01.007 (2022).
9 Taylor, A. M. *et al.* Genomic and Functional Approaches to Understanding Cancer Aneuploidy. *Cancer Cell* **33**, 676-689 e673, doi:10.1016/j.ccell.2018.03.007 (2018).
10 Widschwendter, M. *et al.* Epigenome-based cancer risk prediction: rationale, opportunities and challenges. *Nat Rev Clin Oncol* **15**, 292-309, doi:10.1038/nrclinonc.2018.30 (2018).
11 Yizhak, K. *et al.* RNA sequence analysis reveals macroscopic somatic clonal expansion across normal tissues. *Science* **364**, doi:10.1126/science.aaw0726 (2019).
12 Zhang, S. *et al.* Tumor initiation and early tumorigenesis: molecular mechanisms and interventional targets. *Signal Transduct Target Ther* **9**, 149, doi:10.1038/s41392-024-01848-7 (2024).
13 Kakiuchi, N. & Ogawa, S. Clonal expansion in non-cancer tissues. *Nat Rev Cancer* **21**, 239-256, doi:10.1038/s41568-021-00335-3 (2021).
14 Calderwood, S. K., Khaleque, M. A., Sawyer, D. B. & Ciocca, D. R. Heat shock proteins in cancer: chaperones of tumorigenesis. *Trends Biochem Sci* **31**, 164-172, doi:10.1016/j.tibs.2006.01.006 (2006).
15 Mosser, D. D. & Morimoto, R. I. Molecular chaperones and the stress of oncogenesis. *Oncogene* **23**, 2907-2918, doi:10.1038/sj.onc.1207529 (2004).
16 Cao, L. *et al.* Downregulation of HSPA2 inhibits proliferation via ERK1/2 pathway and endoplasmic reticular stress in lung adenocarcinoma. *Ann Transl Med* **7**, 540, doi:10.21037/atm.2019.10.16 (2019).
17 Huesca, M., Goodwin, A., Bhagwansingh, A., Hoffman, P. & Lingwood, C. A. Characterization of an acidic-pH-inducible stress protein (hsp70), a putative sulfatide binding adhesin, from Helicobacter pylori. *Infect Immun* **66**, 4061-4067, doi:10.1128/IAI.66.9.4061-4067.1998 (1998).
18 Liu, H. *et al.* HSP70 inhibition suppressed glioma cell viability during hypoxia/reoxygenation by inhibiting the ERK1/2 and PI3K/AKT signaling pathways. *J Bioenerg Biomembr* **53**, 405-413, doi:10.1007/s10863-021-09904-5 (2021).
19 Murphy, M. E. The HSP70 family and cancer. *Carcinogenesis* **34**, 1181-1188, doi:10.1093/carcin/bgt111 (2013).
20 Park, H. S., Lee, J. S., Huh, S. H., Seo, J. S. & Choi, E. J. Hsp72 functions as a natural inhibitory protein of c-Jun N-terminal kinase. *EMBO J* **20**, 446-456, doi:10.1093/emboj/20.3.446 (2001).
21 Rohde, M. *et al.* Members of the heat-shock protein 70 family promote cancer cell growth by distinct mechanisms. *Genes Dev* **19**, 570-582, doi:10.1101/gad.305405 (2005).
22 Song, J., Takeda, M. & Morimoto, R. I. Bag1-Hsp70 mediates a physiological stress signalling pathway that regulates Raf-1/ERK and cell growth. *Nat Cell Biol* **3**, 276-282, doi:10.1038/35060068 (2001).
23 Vostakolaei, M. A. *et al.* Hsp70 in cancer: A double agent in the battle between survival and death. *J Cell Physiol* **236**, 3420-3444, doi:10.1002/jcp.30132 (2021).
24 Park, H. S. *et al.* Heat shock protein hsp72 is a negative regulator of apoptosis signal-regulating kinase 1. *Mol Cell Biol* **22**, 7721-7730, doi:10.1128/MCB.22.22.7721-7730.2002 (2002).

25 Ravagnan, L. *et al.* Heat-shock protein 70 antagonizes apoptosis-inducing factor. *Nat Cell Biol* **3**, 839-843, doi:10.1038/ncb0901-839 (2001).
26 Saleh, A., Srinivasula, S. M., Balkir, L., Robbins, P. D. & Alnemri, E. S. Negative regulation of the Apaf-1 apoptosome by Hsp70. *Nat Cell Biol* **2**, 476-483, doi:10.1038/35019510 (2000).
27 Stankiewicz, A. R., Lachapelle, G., Foo, C. P., Radicioni, S. M. & Mosser, D. D. Hsp70 inhibits heat-induced apoptosis upstream of mitochondria by preventing Bax translocation. *J Biol Chem* **280**, 38729-38739, doi:10.1074/jbc.M509497200 (2005).
28 Arya, R., Mallik, M. & Lakhotia, S. C. Heat shock genes - integrating cell survival and death. *J Biosci* **32**, 595-610, doi:10.1007/s12038-007-0059-3 (2007).
29 Srivastava, S., Vishwanathan, V., Birje, A., Sinha, D. & D'Silva, P. Evolving paradigms on the interplay of mitochondrial Hsp70 chaperone system in cell survival and senescence. *Crit Rev Biochem Mol Biol* **54**, 517-536, doi:10.1080/10409238.2020.1718062 (2019).
30 Evans, C. G., Chang, L. & Gestwicki, J. E. Heat shock protein 70 (hsp70) as an emerging drug target. *J Med Chem* **53**, 4585-4602, doi:10.1021/jm100054f (2010).
31 Patury, S., Miyata, Y. & Gestwicki, J. E. Pharmacological targeting of the Hsp70 chaperone. *Curr Top Med Chem* **9**, 1337-1351, doi:10.2174/156802609789895674 (2009).
32 Powers, M. V. *et al.* Targeting HSP70: the second potentially druggable heat shock protein and molecular chaperone? *Cell Cycle* **9**, 1542-1550, doi:10.4161/cc.9.8.11204 (2010).
33 Goloudina, A. R., Demidov, O. N. & Garrido, C. Inhibition of HSP70: a challenging anti-cancer strategy. *Cancer Lett* **325**, 117-124, doi:10.1016/j.canlet.2012.06.003 (2012).
34 Sherman, M. Y. & Gabai, V. L. Hsp70 in cancer: back to the future. *Oncogene* **34**, 4153-4161, doi:10.1038/onc.2014.349 (2015).
35 Singh, G., Chakraborty, S. & Lakhotia, S. C. Elevation of major constitutive heat shock proteins is heat shock factor independent and essential for establishment and growth of Lgl loss and Yorkie gain-mediated tumors in Drosophila. *Cell Stress Chaperones* **27**, 431-448, doi:10.1007/s12192-022-01283-z (2022).
36 Rudrapatna, V. A., Cagan, R. L. & Das, T. K. Drosophila cancer models. *Dev Dyn* **241**, 107-118, doi:10.1002/dvdy.22771 (2012).
37 Leu, J. I., Pimkina, J., Frank, A., Murphy, M. E. & George, D. L. A small molecule inhibitor of inducible heat shock protein 70. *Mol Cell* **36**, 15-27, doi:10.1016/j.molcel.2009.09.023 (2009).
38 Howe, M. K. *et al.* Identification of an allosteric small-molecule inhibitor selective for the inducible form of heat shock protein 70. *Chem Biol* **21**, 1648-1659, doi:10.1016/j.chembiol.2014.10.016 (2014).
39 Miles, W. O., Dyson, N. J. & Walker, J. A. Modeling tumor invasion and metastasis in Drosophila. *Dis Model Mech* **4**, 753-761, doi:10.1242/dmm.006908 (2011).
40 Rossi, F. & Gonzalez, C. Studying tumor growth in Drosophila using the tissue allograft method. *Nat Protoc* **10**, 1525-1534, doi:10.1038/nprot.2015.096 (2015).
41 Campbell, K. *et al.* Collective cell migration and metastases induced by an epithelial-to-mesenchymal transition in Drosophila intestinal tumors. *Nat Commun* **10**, 2311, doi:10.1038/s41467-019-10269-y (2019).
42 Wu, C. Heat shock transcription factors: structure and regulation. *Annu Rev Cell Dev Biol* **11**, 441-469, doi:10.1146/annurev.cb.11.110195.002301 (1995).
43 Puustinen, M. C. & Sistonen, L. Molecular Mechanisms of Heat Shock Factors in Cancer. *Cells* **9**, doi:10.3390/cells9051202 (2020).
44 Mendillo, M. L. *et al.* HSF1 drives a transcriptional program distinct from heat shock to support highly malignant human cancers. *Cell* **150**, 549-562, doi:10.1016/j.cell.2012.06.031 (2012).
45 Scherz-Shouval, R. *et al.* The reprogramming of tumor stroma by HSF1 is a potent enabler of malignancy. *Cell* **158**, 564-578, doi:10.1016/j.cell.2014.05.045 (2014).

46 Huang, W. J. *et al.* Transcriptional upregulation of HSP70-2 by HIF-1 in cancer cells in response to hypoxia. *Int J Cancer* **124**, 298-305, doi:10.1002/ijc.23906 (2009).
47 Donovan, M. R. & Marr, M. T., 2nd. dFOXO Activates Large and Small Heat Shock Protein Genes in Response to Oxidative Stress to Maintain Proteostasis in Drosophila. *J Biol Chem* **291**, 19042-19050, doi:10.1074/jbc.M116.723049 (2016).
48 Parra, A. S. & Johnston, C. A. Mud Loss Restricts Yki-Dependent Hyperplasia in Drosophila Epithelia. *J Dev Biol* **8**, doi:10.3390/jdb8040034 (2020).
49 Essers, M. A. *et al.* FOXO transcription factor activation by oxidative stress mediated by the small GTPase Ral and JNK. *EMBO J* **23**, 4802-4812, doi:10.1038/sj.emboj.7600476 (2004).
50 Wang, M. C., Bohmann, D. & Jasper, H. JNK extends life span and limits growth by antagonizing cellular and organism-wide responses to insulin signaling. *Cell* **121**, 115-125, doi:10.1016/j.cell.2005.02.030 (2005).
51 Luboff, A. J. & DeRemer, D. L. Capivasertib: A Novel AKT Inhibitor Approved for Hormone-Receptor-Positive, HER-2-Negative Metastatic Breast Cancer. *Ann Pharmacother* **58**, 1229-1237, doi:10.1177/10600280241241531 (2024).
52 Xiong, B. *et al.* NOX Family: Regulators of Reactive Oxygen Species Balance in Tumor Cells. *FASEB J* **39**, e70565, doi:10.1096/fj.202500238RRR (2025).
53 Adler, V. *et al.* Regulation of JNK signaling by GSTp. *EMBO J* **18**, 1321-1334, doi:10.1093/emboj/18.5.1321 (1999).
54 Wilhelm, D., Bender, K., Knebel, A. & Angel, P. The level of intracellular glutathione is a key regulator for the induction of stress-activated signal transduction pathways including Jun N-terminal protein kinases and p38 kinase by alkylating agents. *Mol Cell Biol* **17**, 4792-4800, doi:10.1128/MCB.17.8.4792 (1997).
55 Okamura, T. *et al.* Phosphorylation of Glutathione S-Transferase P1 (GSTP1) by Epidermal Growth Factor Receptor (EGFR) Promotes Formation of the GSTP1-c-Jun N-terminal kinase (JNK) Complex and Suppresses JNK Downstream Signaling and Apoptosis in Brain Tumor Cells. *J Biol Chem* **290**, 30866-30878, doi:10.1074/jbc.M115.656140 (2015).
56 Lavoie, S. *et al.* Glutathione precursor, N-acetyl-cysteine, improves mismatch negativity in schizophrenia patients. *Neuropsychopharmacology* **33**, 2187-2199, doi:10.1038/sj.npp.1301624 (2008).
57 Daugaard, M., Rohde, M. & Jaattela, M. The heat shock protein 70 family: Highly homologous proteins with overlapping and distinct functions. *FEBS Lett* **581**, 3702-3710, doi:10.1016/j.febslet.2007.05.039 (2007).
58 Schmidt, E. E. *et al.* GenomeRNAi: a database for cell-based and in vivo RNAi phenotypes, 2013 update. *Nucleic Acids Res* **41**, D1021-1026, doi:10.1093/nar/gks1170 (2013).
59 Rosenzweig, R., Nillegoda, N. B., Mayer, M. P. & Bukau, B. The Hsp70 chaperone network. *Nat Rev Mol Cell Biol* **20**, 665-680, doi:10.1038/s41580-019-0133-3 (2019).
60 Ciocca, D. R. *et al.* Heat shock protein hsp70 in patients with axillary lymph node-negative breast cancer: prognostic implications. *J Natl Cancer Inst* **85**, 570-574, doi:10.1093/jnci/85.7.570 (1993).
61 Syrigos, K. N. *et al.* Clinical significance of heat shock protein-70 expression in bladder cancer. *Urology* **61**, 677-680, doi:10.1016/s0090-4295(02)02289-6 (2003).
62 Zhao, K. *et al.* HSP70 Family in Cancer: Signaling Mechanisms and Therapeutic Advances. *Biomolecules* **13**, doi:10.3390/biom13040601 (2023).
63 Rangel, D. F. *et al.* Endoplasmic reticulum chaperone GRP78/BiP is critical for mutant Kras-driven lung tumorigenesis. *Oncogene* **40**, 3624-3632, doi:10.1038/s41388-021-01791-9 (2021).
64 Shen, J. *et al.* GRP78 haploinsufficiency suppresses acinar-to-ductal metaplasia, signaling, and mutant Kras-driven pancreatic tumorigenesis in mice. *Proc Natl Acad Sci U S A* **114**, E4020-E4029, doi:10.1073/pnas.1616060114 (2017).

65 Fu, Y. *et al.* Pten null prostate tumorigenesis and AKT activation are blocked by targeted knockout of ER chaperone GRP78/BiP in prostate epithelium. *Proc Natl Acad Sci U S A* **105**, 19444-19449, doi:10.1073/pnas.0807691105 (2008).
66 Liu, P., Cheng, H., Roberts, T. M. & Zhao, J. J. Targeting the phosphoinositide 3-kinase pathway in cancer. *Nat Rev Drug Discov* **8**, 627-644, doi:10.1038/nrd2926 (2009).
67 Xu, F. *et al.* HSP70 inhibitor VER155008 suppresses pheochromocytoma cell and xenograft growth by inhibition of PI3K/AKT/mTOR and MEK/ERK pathways. *Int J Clin Exp Pathol* **12**, 2585-2594 (2019).
68 Gong, S., Zhang, Y., Tian, A. & Deng, W. M. Tumor models in various Drosophila tissues. *WIREs Mech Dis* **13**, e1525, doi:10.1002/wsbm.1525 (2021).
69 Cobreros, L., Fernandez-Minan, A., Luque, C. M., Gonzalez-Reyes, A. & Martin-Bermudo, M. D. A role for the chaperone Hsp70 in the regulation of border cell migration in the Drosophila ovary. *Mech Dev* **125**, 1048-1058, doi:10.1016/j.mod.2008.07.006 (2008).
70 Liao, Y. *et al.* Higher heat shock factor 1 expression in tumor stroma predicts poor prognosis in esophageal squamous cell carcinoma patients. *J Transl Med* **13**, 338, doi:10.1186/s12967-015-0703-x (2015).
71 Kourtis, N. *et al.* Oncogenic hijacking of the stress response machinery in T cell acute lymphoblastic leukemia. *Nat Med* **24**, 1157-1166, doi:10.1038/s41591-018-0105-8 (2018).
72 Chen, R., Liliental, J. E., Kowalski, P. E., Lu, Q. & Cohen, S. N. Regulation of transcription of hypoxia-inducible factor-1alpha (HIF-1alpha) by heat shock factors HSF2 and HSF4. *Oncogene* **30**, 2570-2580, doi:10.1038/onc.2010.623 (2011).
73 Forsythe, J. A. *et al.* Activation of vascular endothelial growth factor gene transcription by hypoxia-inducible factor 1. *Mol Cell Biol* **16**, 4604-4613, doi:10.1128/MCB.16.9.4604 (1996).
74 Greer, E. L. & Brunet, A. FOXO transcription factors at the interface between longevity and tumor suppression. *Oncogene* **24**, 7410-7425, doi:10.1038/sj.onc.1209086 (2005).
75 Zhang, Y., Gan, B., Liu, D. & Paik, J. H. FoxO family members in cancer. *Cancer Biol Ther* **12**, 253-259, doi:10.4161/cbt.12.4.15954 (2011).
76 Shao, D. *et al.* A functional interaction between Hippo-YAP signalling and FoxO1 mediates the oxidative stress response. *Nat Commun* **5**, 3315, doi:10.1038/ncomms4315 (2014).
77 Perez, E., Lindblad, J. L. & Bergmann, A. Tumor-promoting function of apoptotic caspases by an amplification loop involving ROS, macrophages and JNK in Drosophila. *Elife* **6**, doi:10.7554/eLife.26747 (2017).
78 Enomoto, M. & Igaki, T. Deciphering tumor-suppressor signaling in flies: genetic link between Scribble/Dlg/Lgl and the Hippo pathways. *J Genet Genomics* **38**, 461-470, doi:10.1016/j.jgg.2011.09.005 (2011).
79 Wu, J. S. & Luo, L. A protocol for mosaic analysis with a repressible cell marker (MARCM) in Drosophila. *Nat Protoc* **1**, 2583-2589, doi:10.1038/nprot.2006.320 (2006).
80 Ray, M., Singh, G. & Lakhotia, S. C. Altered levels of hsromega lncRNAs further enhance Ras signaling during ectopically activated Ras induced R7 differentiation in Drosophila. *Gene Expr Patterns* **33**, 20-36, doi:10.1016/j.gep.2019.05.002 (2019).
81 Woodhouse, E., Hersperger, E. & Shearn, A. Growth, metastasis, and invasiveness of Drosophila tumors caused by mutations in specific tumor suppressor genes. *Dev Genes Evol* **207**, 542-550, doi:10.1007/s004270050145 (1998).

Figure Legends

Fig 1. Hsp70 is expressed in a progressive spatio-temporal pattern in developing tumours.

(**A-D**) Confocal projection images of wing imaginal discs with *lgl*^{4} *yki*^{OE} (green) clones at 72 h, 96h, 120h, 144h ACI, showing stage specific expression and distribution of Hsp70 (red). Scale bar 50 µm. (**E-F**) Dot-bar plots (Y-axis on left) and line graphs (Y-axis on right) showing increased Hsp70 distribution (E) and intensity (F) within clonal area over time. (n = as indicated at the base of each bar). (**G-I**) Effect of *hsp70* downregulation on clonal growth of *lgl*^{4} *yki*^{OE} (green) discs at 72 h, 96h, 120h ACI. Scale bar 50 µm. (**J**) Dot-bar plot showing reduced clonal area in *lgl*^{4} *yki*^{OE}; *hsp70*^{RNAi} discs (blue) compared to *lgl*^{4} *yki*^{OE} (gray) across time-points (n = as indicated on top of each bar), corresponding to panels A-G. (**K**) Bar graph showing relative reduction in Hsp70 levels in *lgl*^{4} *yki*^{OE}; *hsp70*^{RNAi} wing discs (n = 24) compared to in *lgl*^{4} *yki*^{OE} controls (n = 30) at 96 h ACI. *p < 0.05, **p < 0.01, ***p < 0.001; ns = not significant (p > 0.05); unpaired Student's t-test. (**L**) Schematic summarizing clonal growth and Hsp70 expression in *lgl*^{4} *yki*^{OE} and *lgl*^{4} *yki*^{OE}; *hsp70 RNAi* background.

Fig 2. Alterations in Hsp70 levels regress growth and survivability of tumour cells

(**A-C**) Confocal projections of *lgl*^{4} *yki*^{OE} clones (green) at 72 h ACI showing mitotic index through number of pH3+ nuclei (grey), compared to *lgl*^{4} *yki*^{OE}; *hsp70*^{RNAi} clones. Scale bar: 50 µm. The number of pH3+ foci were quantified and represented as a scatter plot (n = 65), p<0.0001 (C). (**D-F**) Confocal projections showing Dcp-1 staining (white) within *lgl*^{4} *yki*^{OE} and *lgl*^{4} *yki*^{OE}; *hsp70*^{RNAi} clones (green) at 72 h ACI, Scale bar: 50 µm. The relative Dcp-1 intensity among the samples were represented as violin plot (n =146 *lgl*^{4} *yki*^{OE} clones, n = 64 *lgl*^{4} *yki*^{OE}; *hsp70*^{RNAi} clones), ***p < 0.001, unpaired Student's t- test (F). (**G**) Stacked bar graph showing percentages (± S.E.) of pseudopupae, pharate, and adult survivors in *lgl*^{4} *yki*^{OE} and *lgl*^{4} *yki*^{OE}; *hsp70*^{RNAi} tumour-bearing backgrounds (n = 200 larvae of each genotype), *p<0.05, **p < 0.01, unpaired Student's t- test. (**H-J**) Confocal images showing GFP+ *lgl*^{4} *yki*^{OE} clones in untreated (UT) and 24 h Pifithrin-µ (PFT-µ) treated larval discs at 72 h ACI (Scale bar: 50 µm), further quantified and represented as mean ± s.e.m, n = 18 (UT), n = 16 (PFT-µ), ***p < 0.001 (J). (**K**) Stacked bar graph comparing developmental outcomes (% death as pseudopupae, pharate adults, and adult emergence) between untreated and PFT-µ-treated *lgl*^{4} *yki*^{OE} larvae (n = 50 larvae in each treatment group). (**L-M**) Frequency of tumour nodules, as shown in the

representative image (J), present in different parts of the surviving adult flies that bore *lgl*^{4} *yki*^{OE} or *lgl*^{4} *yki*^{OE}; *hsp70*^{RNAi} tumour clones.

Fig 3. Hsp70 expressing *lgl*^{4} *yki*^{OE} tumour cells show enhanced invasive phenotypes.

(**A-D**) Confocal projection images of wing disc bearing *lgl*^{4} *yki*^{OE} and *lgl*^{4} *yki*^{OE}; *hsp70*^{RNAi} clones at 72 h ACI, showing MMP1 expression within the clonal regions. Scale bar: 50 µm. MMP1 intensity was quantified and represented as fold change correlating with the clonal area. (n =15 (MMP1), n = 13 (clonal area)), ***p < 0.001, unpaired Student's t- test (D). (**E**) Confocal projection across three optical planes of *lgl*^{4} *yki*^{OE} clones at 96 h ACI, showing shape of GFP^{+} Hsp70^{+} tumour cells, Scale bar: 1 µm. (**F-G**) Confocal optical section depicting unilateral F-actin distribution (Phalloidin) (white arrows) at the junction of Hsp70 high and low expressing cells (F') Scale bar: 2 µm. (**H**) Quantitative disc plot showing directional bias of Hsp70^{+} cells in *lgl*^{4} *yki*^{OE} tumours (n = 15 clones from 10 discs).

Fig 4. Enhanced invasiveness of *lgl*^{4} *yki*^{OE} tumour allografts in *OregonR*$^{+}$ flies is dependent on Hsp70.

(**A**) Schematic depicting the wing tumour transplantation procedure in *Drosophila*. (**B-D**) Relative abdominal distension in the host flies (*OregonR*$^{+}$) when their abdomens were grafted with *lgl*^{4} *yki*^{OE}, *lgl*^{4} *yki*^{OE}; *hsp70*^{RNAi} compared to control. (**E-F**) Progressive increase in size of the disc grafts of *lgl*^{4} *yki*^{OE} (E) and *lgl*^{4} *yki*^{OE}; *hsp70*^{RNAi} (F) within the host abdomen over the indicated time periods, as shown by enhancement of GFP fluorescence. (**G**) Quantification of abdominal area corresponding to panels B–D (n = 5 for *lgl*^{4} *yki*^{OE} and *OregonR*$^{+}$, n = 6 for *lgl*^{4} *yki*^{OE}; *hsp70*^{RNAi}), **p < 0.01, unpaired Student t-test. (**H**) Mean fluorescence intensity (MFI) of GFP signal from host abdomens over time (panels E–F). (**I-L**) Confocal images at day 14 post-transplantation showing (I) overgrown GFP+ tumour mass (I), local invasion into nearby muscle tissue (magenta) (J) and micro-metastases in surrounding tissues marked by GFP^{+} Hsp70^{+} cells (yellow; white arrows) (K–L). Scale bar: 50 µm.

Fig 5. Non-canoncial induction of Hsp70 in *lgl*^{4} *yki* ^{OE} tumours.

(**A-B**) Confocal optical sections showing HSF (white) and Hsp70 (red) expression in clonal (GFP^{+}, green) and non-clonal (grey) areas of *lgl*^{4} *yki*^{OE} and *lgl*^{4} *yki*^{OE}, *hsf*^{RNAi} tumour discs at 72 h ACI. Scale bar: 50 µm. (**C-E**) Quantification of HSF intensity ratio between clonal and non-clonal regions. Ratiometric change in HSF intensity among the clonal and non-clonal area (E), reflected by its unchanged pattern in *lgl*^{4} *yki*^{OE} (C) and significant reduction in its clonal intensity compared to non-clonal regions (D), (n = 46), ***p < 0.001. (**F–H**) Quantification of Hsp70 distribution (F), intensity (G) within clonal regions and the total clonal area (H) between the indicated genotypes, n = 19, ns – not-significant. (**I**) Stacked bar graphs comparing developmental outcomes (pseudopupae, pharate, and adult stages) in *lgl*^{4} *yki*^{OE}, *hsf*^{RNAi} compared to *lgl*^{4} *yki*^{OE} (n = 120 larvae), ***p < 0.001. (**J**) Digitally zoomed confocal optical section showing distribution of FOXO and Hsp70 in *lgl*^{4} *yki*^{OE} clones (green) at 72 h ACI. (**K–L**) Confocal images of *lgl*^{4} *yki*^{OE} and *lgl*^{4} *yki*^{OE}*; dfoxo*^{RNAi} tumour discs showing GFP^{+} clones and Hsp70 expression. Scale bar: 50 µm. (**M–O**) Quantification plots showing Hsp70 intensity, percentage of clonal area covered by Hsp70 and overall clonal size in the indicated genotypes. (n = 22) ***p < 0.001. (**P**) Stacked bar graphs comparing developmental outcomes (pseudopupae, pharate, and adult stages) in *lgl*^{4} *yki*^{OE}*; dfoxo*^{RNAi} compared to *lgl*^{4} *yki*^{OE} (n = 300 larvae), ***p < 0.001.

Fig 6. JNK activated FOXO mediates Hsp70 expression.

(**A–B**) Confocal projection images showing GFP+ clones and Hsp70 expression in untreated (A) and Capivasertib-treated (B) *lgl*^{4} *yki*^{OE} tumourous wing discs at 72 hr ACI + 24 hr after drug treatment. Scale bar: 50 µm. (**C-E**) Quantification of clonal area in Capivasertib-treated discs (C), Hsp70 distribution (D) and intensity (E) compared to untreated (UT) controls (n = 13). (**F-G**) Confocal projections showing GFP+ clonal area and Hsp70 expression in *lgl*^{4} *yki*^{OE} (F) versus *lgl*^{4} *yki*^{OE}*; UAS- bsk*^{DN} (G) tumour discs. Scale bar: 50 µm. (**H-J**) Plots showing quantification of clonal area (H), Hsp70 intensity (I) and clonal area covered by Hsp70 (J) in *lgl*^{4} *yki*^{OE}*; UAS- bsk*^{DN} tumours compared to *lgl*^{4} *yki*^{OE} controls (n = 19). *p < 0.05, **p < 0.01, ***p < 0.001, ns – non-significant p > 0.05, unpaired Student's t-test.

Fig 7. Activation of Hsp70 via FOXO is redox-regulated.

(**A–B**) Confocal optical sections showing GFP+ clones and Hsp70 expression in *lgl*^{4} *yki*^{OE} (A) and *lgl*^{4} *yki*^{OE}*; nox*^{RNAi} (B) tumour discs at 72 hr ACI. Scale bar: 50 µm. (**C-E**) Quantification plots denoting changes in clonal area (C), Hsp70 coverage of the clonal area (D) and its expression level (E) in *lgl*^{4} *yki*^{OE}*; nox*^{RNAi} tumours (n = 16) compared to controls (n = 14). (**F**) Graph showing changes in pJNK intensity within clonal areas of *lgl*^{4} *yki*^{OE}*; nox*^{RNAi} discs compared to *lgl*^{4} *yki*^{OE} tumours (n = 157 clones). (**G**) Stacked bar graph showing developmental outcomes (pseudopupae, pharate, and adult stages) in *lgl*^{4} *yki*^{OE} vs. *lgl*^{4} *yki*^{OE}*; nox*^{RNAi} tumours (n = 270 larvae of each genotype). (**H–I**) Confocal images of *lgl*^{4} *yki*^{OE} tumour discs showing GFP+ clones and Hsp70 expression in untreated (H) and Buthionine sulfoximine (BSO)-treated (I) larvae. Scale bar: 50 µm. (**J-L**) Plots showing changes in clonal area (J), Hsp70 expression (K) and its distribution within the clones (L), in BSO treated *lgl*^{4} *yki*^{OE} larvae (n = 27) over untreated (UT) controls (n = 22). (**M**) pJNK intensity in BSO-treated *lgl*^{4} *yki*^{OE} tumours compared to untreated controls (n = 62 clones). *$p < 0.05$, **$p < 0.01$, ***$p < 0.001$, ****$p < 0.0001$, unpaired Student t-test. Representative image in shown in Fig S6A.

Figure 1

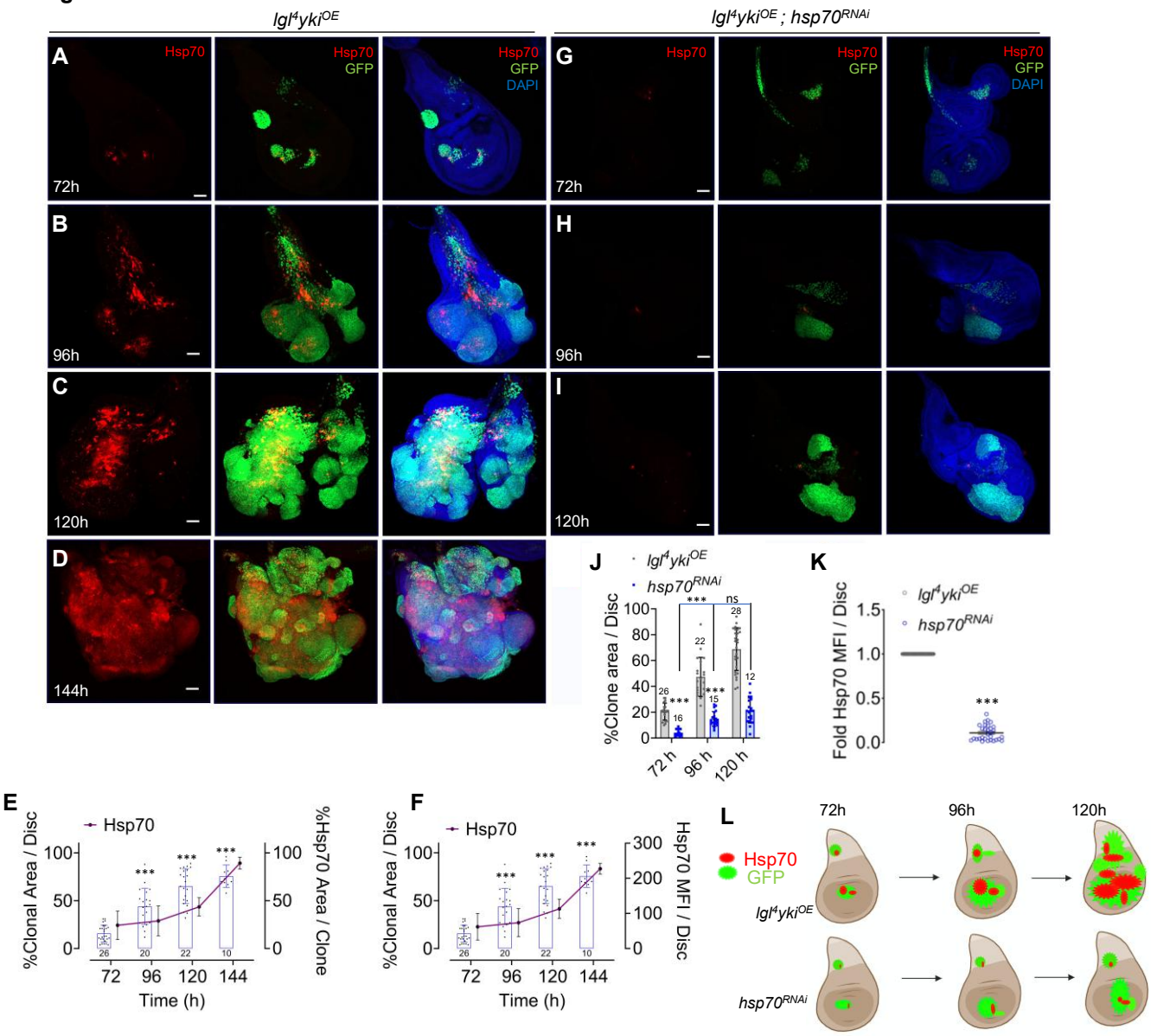
lgl4ykiOE
lgl4ykiOE ; hsp70RNAi
A
Hsp70
Hsp70
GFP
Hsp70
GFP
DAPI
72h
B
96h
C
120h
D
144h
G
H
I
J
lgl4ykiOE
hsp70RNAi
%Clone area / Disc
72 h
96 h
120 h
ns
K
Fold Hsp70 MFI / Disc
E
Hsp70
%Clonal Area / Disc
%Hsp70 Area / Clone
Time (h)
F
Hsp70 MFI / Disc
L
Hsp70
GFP
lgl4ykiOE
hsp70RNAi

Figure 2

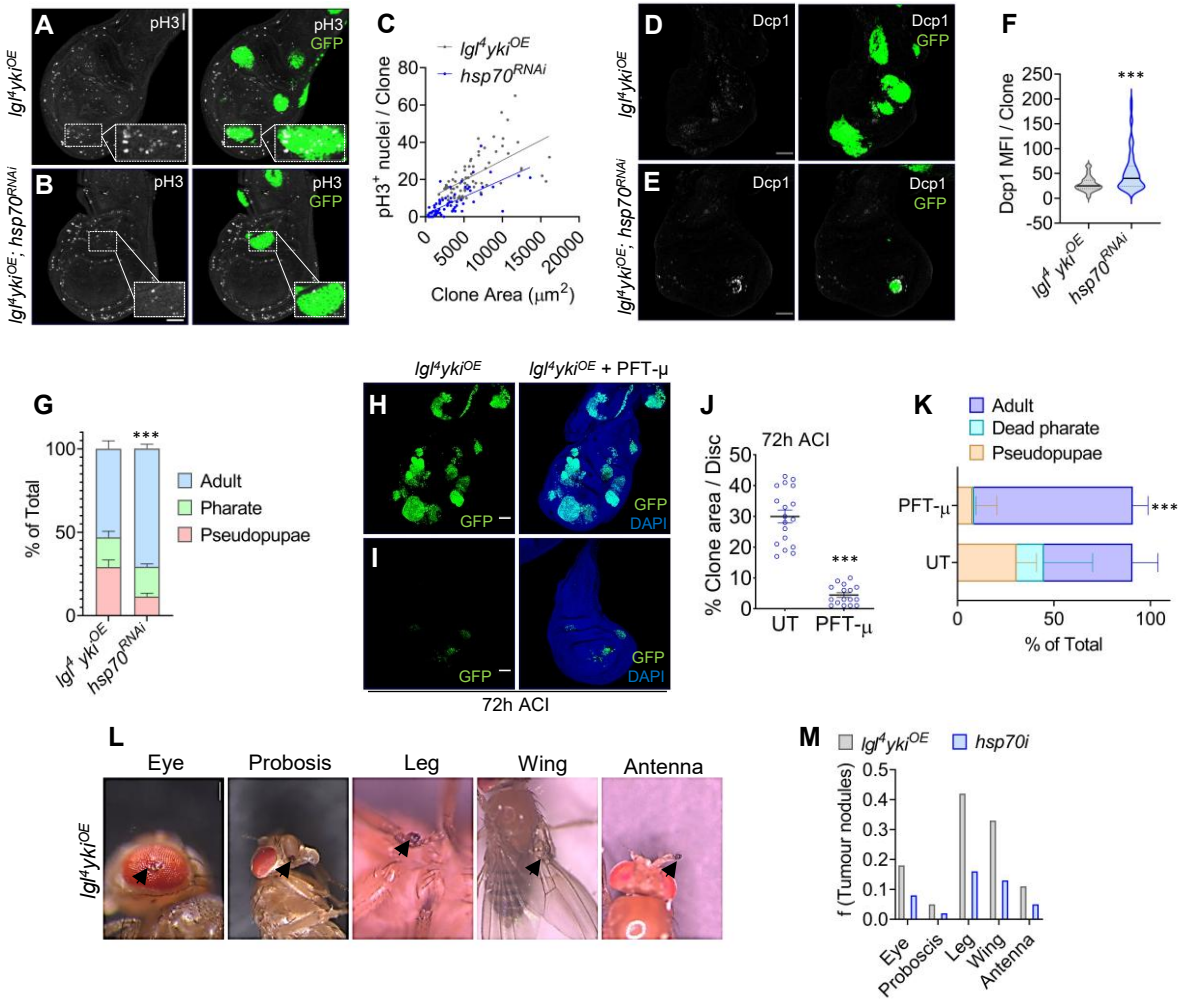
A
pH3
pH3
GFP
lgl4ykiOE
B
pH3
pH3
GFP
lgl4ykiOE; hsp70RNAi
C
lgl4ykiOE
hsp70RNAi
pH3+ nuclei / Clone
Clone Area (μm2)
D
Dcp1
Dcp1
GFP
E
Dcp1
Dcp1
GFP
F
Dcp1 MFI / Clone
***
G
% of Total
***
Adult
Pharate
Pseudopupae
H
lgl4ykiOE
lgl4ykiOE + PFT-μ
GFP
GFP
DAPI
I
GFP
GFP
DAPI
72h ACI
J
72h ACI
% Clone area / Disc
***
UT
PFT-μ
K
Adult
Dead pharate
Pseudopupae
PFT-μ
UT
***
% of Total
L
Eye
Probosis
Leg
Wing
Antenna
lgl4ykiOE
M
lgl4ykiOE
hsp70i
f (Tumour nodules)
Eye
Proboscis
Leg
Wing
Antenna

Figure 3

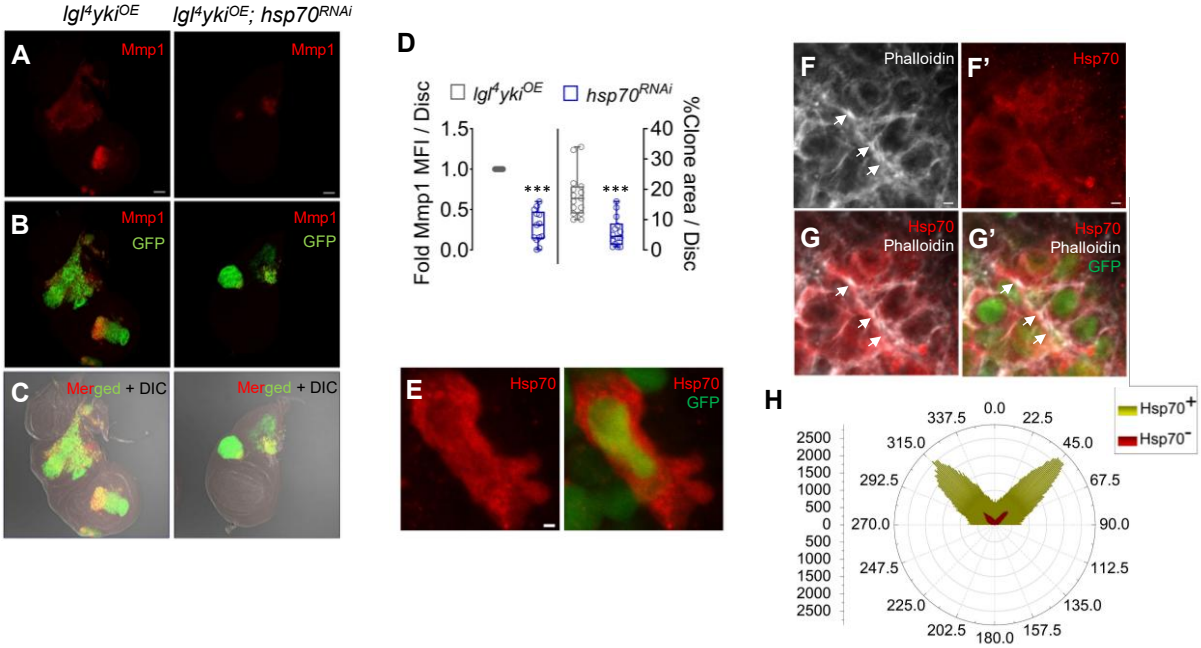
lgl4ykiOE
lgl4ykiOE; hsp70RNAi
A
Mmp1
Mmp1
B
Mmp1
GFP
Mmp1
GFP
C
Merged + DIC
Merged + DIC
D
lgl4ykiOE
hsp70RNAi
Fold Mmp1 MFI / Disc
%Clone area / Disc
1.5
1.0
0.5
0.0
40
30
20
10
0
***
***
E
Hsp70
Hsp70
GFP
F
Phalloidin
F'
Hsp70
G
Hsp70
Phalloidin
G'
Hsp70
Phalloidin
GFP
H
Hsp70+
Hsp70-
0.0
22.5
45.0
67.5
90.0
112.5
135.0
157.5
180.0
202.5
225.0
247.5
270.0
292.5
315.0
337.5
2500
2000
1500
1000
500
0
500
1000
1500
2000
2500

Figure 4

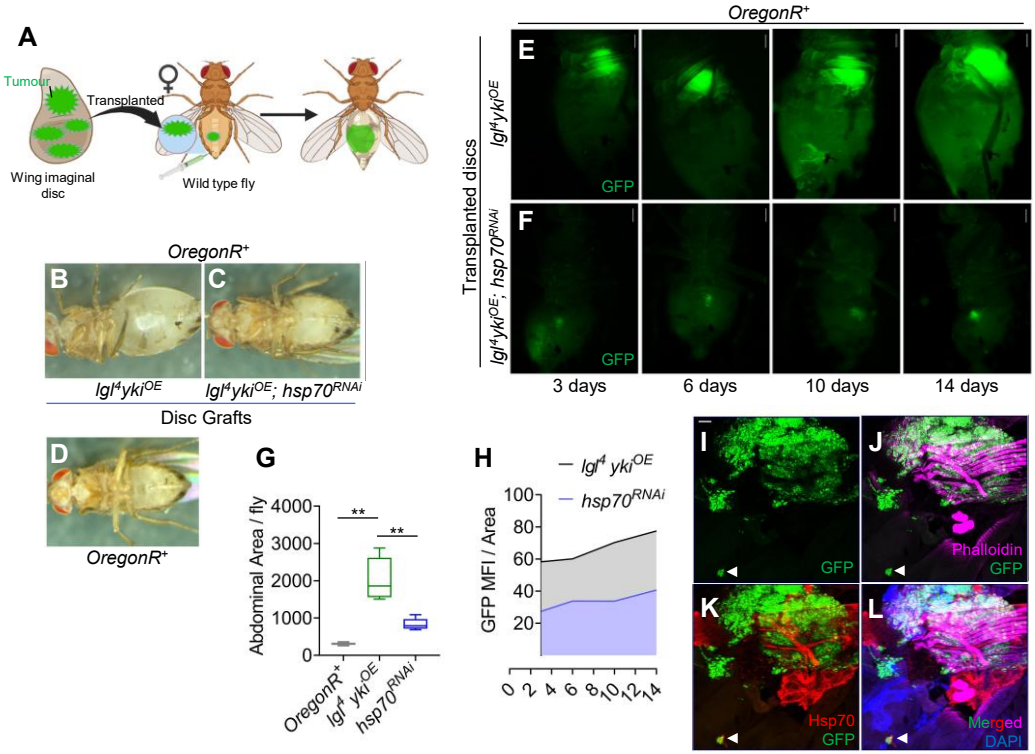
A
Tumour
Transplanted
Wing imaginal disc
Wild type fly
OregonR+
B
C
lgl4ykiOE
lgl4ykiOE; hsp70RNAi
Disc Grafts
D
OregonR+
G
Abdominal Area / fly
4000
3000
2000
1000
0
**
**
OregonR+
lgl4 ykiOE
hsp70RNAi
H
lgl4 ykiOE
hsp70RNAi
GFP MFI / Area
100
80
60
40
20
0 2 4 6 8 10 12 14
OregonR+
Transplanted discs
lgl4ykiOE
lgl4ykiOE; hsp70RNAi
E
F
GFP
3 days
6 days
10 days
14 days
I
J
K
L
GFP
Phalloidin
Hsp70
Merged
DAPI

Figure 5

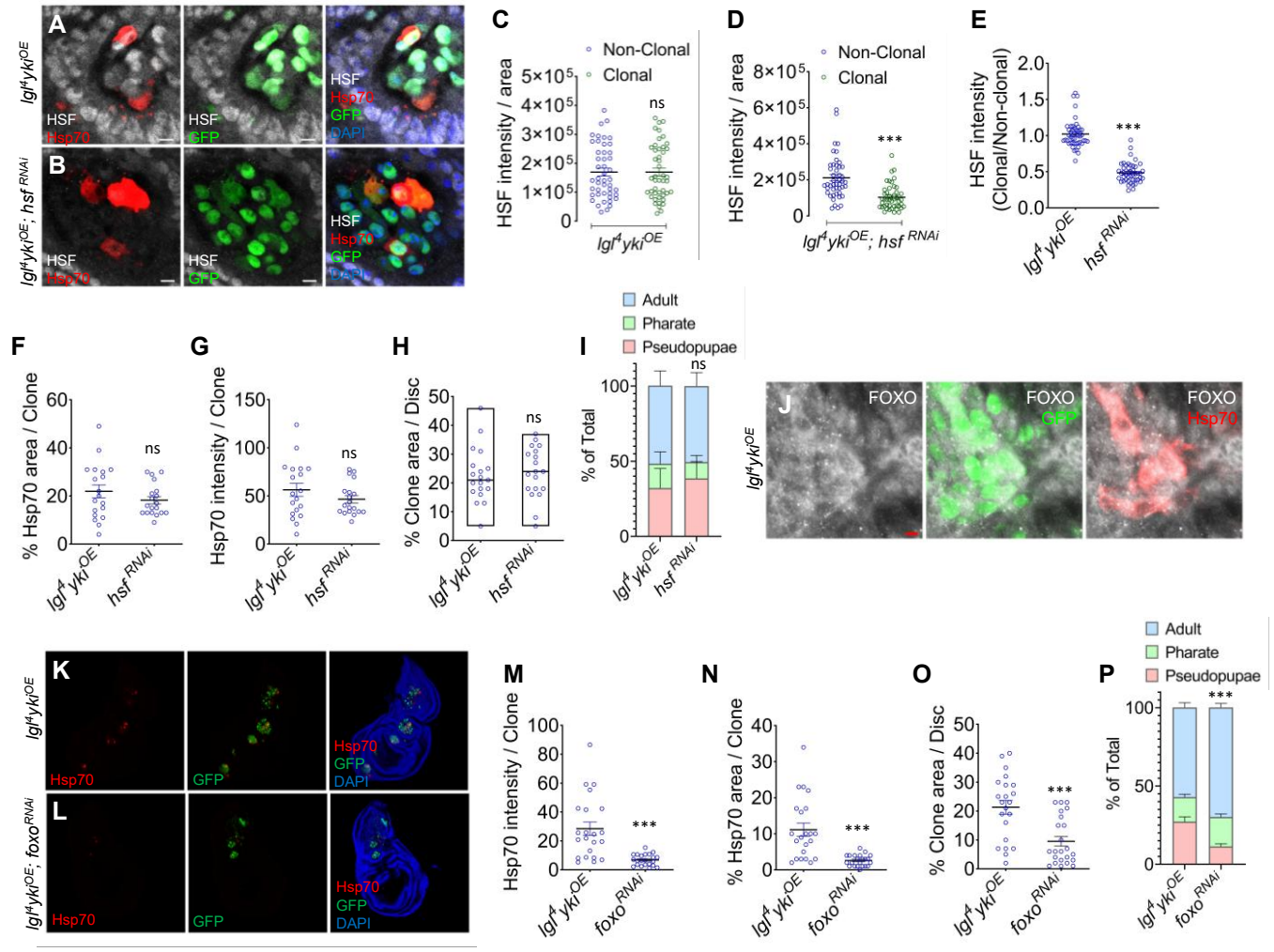
A
B
HSF
Hsp70
GFP
DAPI
C
D
E
Non-Clonal
Clonal
HSF intensity / area
HSF intensity (Clonal/Non-clonal)
ns
***
F
G
H
I
% Hsp70 area / Clone
Hsp70 intensity / Clone
% Clone area / Disc
% of Total
Adult
Pharate
Pseudopupae
J
FOXO
K
L
M
N
O
P

Figure 6

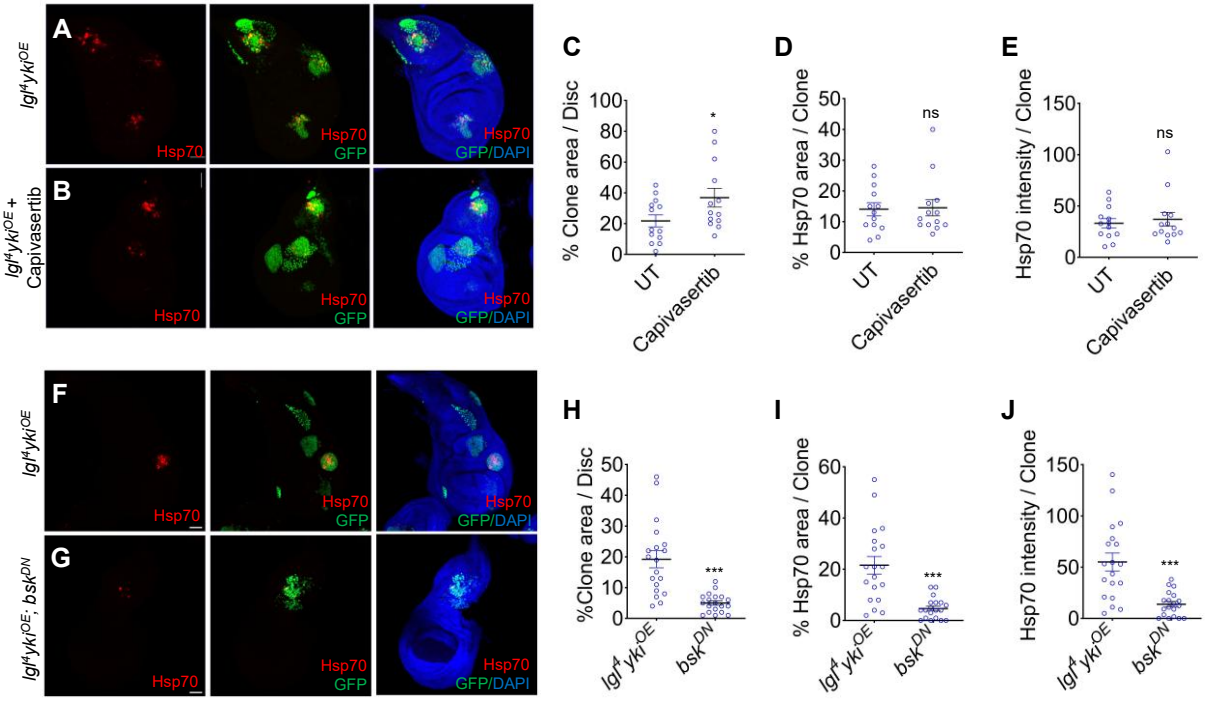
A
B
F
G
Hsp70
GFP
GFP/DAPI
C
D
E
H
I
J
% Clone area / Disc
% Hsp70 area / Clone
Hsp70 intensity / Clone
%Clone area / Disc
UT
Capivasertib
ns
*
***

Figure 7

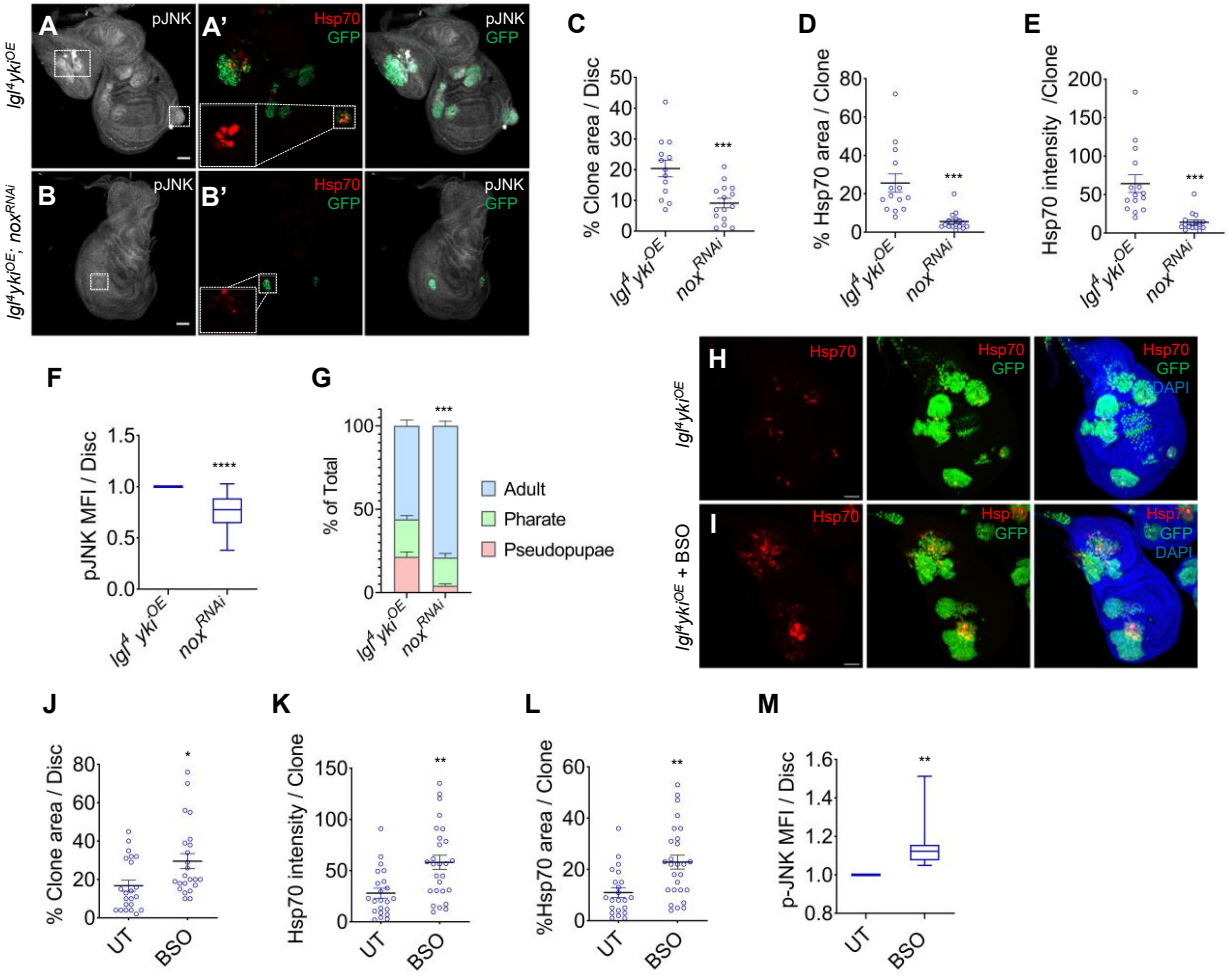
A
pJNK
A'
Hsp70
GFP
pJNK
GFP
B
pJNK
B'
Hsp70
GFP
pJNK
GFP
lgl4ykiOE
lgl4ykiOE; noxRNAi
C
% Clone area / Disc
lgl4 ykiOE
noxRNAi
D
% Hsp70 area / Clone
E
Hsp70 intensity /Clone
F
pJNK MFI / Disc
G
% of Total
Adult
Pharate
Pseudopupae
H
Hsp70
GFP
DAPI
I
lgl4ykiOE + BSO
J
% Clone area / Disc
UT
BSO
K
Hsp70 intensity / Clone
L
%Hsp70 area / Clone
M
p-JNK MFI / Disc